Direct Observation of Polyvinylchloride Degradation in Water at Temperatures up to 500°C and at Pressures up to 700 MPa

Yorihiko Nagai, Richard L. Smith Jr., Hiroshi Inomata, Kunio Arai

Research Center of Supercritical Fluid Technology, Tohoku University, Sendai 980-8579, Japan

Received 9 January 2007; accepted 23 February 2007
DOI 10.1002/app.26790
Published online 8 July 2007 in Wiley InterScience (www.interscience.wiley.com).

ABSTRACT: Degradation of polyvinylchloride (PVC) in high-temperature and supercritical water was studied with a hydrothermal diamond anvil cell to determine phase change characteristics of the reacting polymer with respect to water density. During the reaction period of 500 s, at temperatures between 400 and 500°C and at water densities from 0 to 930 kg/m^3, PVC particles exhibited clearly defined spreading on the anvil surface that was defined as spread time, S_t. The spread times decreased with increasing temperature and the values increased with increasing water density. Analysis of the residues with infrared spectroscopy showed the presence of both polyenes and polyols, whose formation was correlated with water density. From the analyses, nucleophilic substitution of PVC in water was found to be promoted at low temperatures ($\sim$ 400°C) and high water densities (>830 kg/m^3), whereas the ionic chain dechlorination was promoted at high temperatures ($> \sim$ 450°C) and low water densities ($\sim$ 750 kg/m^3). A reaction pathway is proposed that shows —OH nucleophilic substitution in competition with ionic chain reaction for dechlorination both of which vary with water density. © 2007 Wiley Periodicals, Inc. J Appl Polym Sci 106: 1075–1086, 2007

Key words: PVC dechlorination; supercritical water; polyene; polyol; batch microreactor

INTRODUCTION

The origin, growth, and future of polyvinylchloride (PVC) has been summarized by Braun, who noted that PVC will most likely have a steady growth rate in the coming years.[1,2] Indeed, production of PVC has continued to show strong growth in the U.S. and Canada, Europe, Japan, and South Korea, with total production of PVC plastics among these countries being 15.8, 16.4, and 17.1 million metric tons for the years 2001, 2002, and 2003, respectively.[3] Among the plastics produced, PVC represents the second largest product in volume, followed by polyethylene.[4]

Some of the attractive qualities of PVC are related to its excellent low permeability to oxygen and other small molecules, which makes it a suitable material for preventing spoilage associated with food storage, and for preventing the loss of food flavor compounds.[5] For example, the permeability coefficient for PVC with O_2 has a value of 0.034×10^{-13} cm^3/(cm^2 s Pa) at 25°C, compared with values for high-density and low-density polyethylenes that are roughly 8.8 and 64.7 times higher, respectively, making PVC highly desirable and unique among commodity plastics.[6] Because of its utility and increased usage, methods for PVC recycle will become increasingly important in the future.

Braun[4] has summarized some of the waste disposal and recycle options for PVC that include incineration, material recycle, and chemical recycle methods. Disposal of PVC by incineration is convenient and allows for energy recovery, but has the possibility to introduce toxic dioxins or furans into the environment, due to PVC's high (up to 57 wt %) chlorine content.[3] Further, incineration as a waste disposal method in itself carries with it a growing public resistance.[4] On the other hand, Bhaskar et al.[7] have proposed using a method based on staged temperature treatment to prevent the formation of chlorinated hydrocarbon compounds and have demonstrated the technique by studying PVC mixed with plastics such as polystyrene or polyethylene.

Development of chemical recycle methods, where one breaks down polymeric materials into smaller chemical compounds, is essential for recycling plastics in the future. High-temperature water is especially attractive as a solvent for recycling PVC, since PVC is weak towards both heat and water. In the chemical recycle of PVC, it is generally accepted that PVC must be dechlorinated before it is processed further as polymeric units or other compounds. PVC

Correspondence to: R. L. Smith (smith@scf.che.tohoku.ac.jp).

Contract grant sponsor: Japan Chemical Innovation Institute (JCII).

dechlorinates in high-temperature water[8] and also in aqueous caustic solutions.[9] Dechlorination of PVC in concentrated aqueous caustic solutions has been shown to readily occur and this has been demonstrated for industrial grade PVC.[9] Dechlorination of PVC in high-temperature water with and without catalysts or other additives has also been studied and this is discussed next.

Table I summarizes some of the major solid, liquid, and gaseous reaction products identified in the treatment of PVC with water under catalytic and noncatalytic conditions.[10–16] Most of the experiments performed on reaction of PVC in water have used samples having molecular weights around 65,000 for relatively long reaction times. In Table I, the densities shown are either those determined from mass/volume data given in the articles or those calculated from the saturation properties of water.[17] Many of the research works shown in Table I focused on the maximum dechlorination that could be achieved in water. From the available results in Table I, it can be said that for reaction temperatures greater than 300°C, gaseous hydrocarbons and CO_2 are generated, whereas for reaction densities greater than 700 kg/m^3, polyene structures are observed. Further, for the case of liquid products, there seems to be a trend in the formation of ring compounds with either water density or temperature.

In the supercritical region, reaction rates, especially those in water, can be expected to be strong functions of temperature or density, as noted in several reviews.[18–21] At the critical point of water, the liquid density becomes equal to that of the vapor density, or critical density (ρ_c), which has a value of 322.00 kg/m^3 at the critical temperature (T_c), 373.946°C, corresponding to the critical pressure (P_c), 22.064 MPa.[17] As the temperature of water is raised above its critical temperature, T_c, the water density can be varied continuously without phase change between low density (<50 kg/m^3) and high density (>500 kg/m^3) states, as studied in this work. Over these range of water densities, the chemical nature of water changes from one that supports radical reactions at low densities to one that supports ionic reactions at high densities.[22] Many of the interactions of water with simple compounds has been summarized in a review by Watanabe et al.,[22] who point to the properties of water such as density, diffusion coefficient, viscosity, dielectric constant, and ion product as strongly influencing reaction pathways.

Although reaction of PVC in high-temperature water has been studied in a number of works as shown in Table I, few conclusions can be drawn regarding the effect of water density on the PVC degradation process. Phase behavior and changes during the reaction are essentially unknown, which can probably be attributed to the lack of suitable equipment for containing water at conditions of high temperatures and high pressures in addition to practical aspects of reactor materials and corrosion due to the potentially high HCl concentrations generated during the dechlorination reaction. In this work, we used a microreactor that was developed in geological sciences,[23] which has been applied by our group to numerous organic-supercritical water and polymer-supercritical water systems.[24,25] Our objectives in this work were: (i) to determine the phase changes and characteristics of PVC during reaction in high temperature water, (ii) to determine the effect of water density on PVC during reaction, and (iii) to analyze the reacted PVC at relatively short reaction times and discuss possible differences in the reaction pathways according to temperature and density of the aqueous environment.

EXPERIMENTAL

Materials

The PVC used in the experiments was in powder form and was obtained from Aldrich Chemical Co. (St. Louis, MO). The PVC was additive-free and had a molecular weight, M_w, of 62,000 and a number average molecular weight, M_n, of 35,000. The melting temperature, T_m, of the polymer was $\sim$212°C as determined by differential scanning calorimetry. Argon (99.99%) used in the experiments for adjusting the reaction chamber fill densities and argon + 1% hydrogen gas mixtures used for preventing diamond oxidation during heating were obtained from Tanuma Sanso (Sendai, Japan). The water used was double-distilled and had a resistivity greater than 18 MΩ. The diamond anvils used were type Ia, brilliant cut, and had 1-mm culets. AgI used for alignment checks was obtained as a gift from Professor Bassett of Cornell University. Material used for the reactor chamber was Inconel-600 and was obtained from Nilaco Corp. (Tokyo, Japan). Molybdenum oxide wire (0.7 mm diameter) used in the construction of the microheaters was obtained from Nilaco Corp.

Methods

A Bassett type hydrothermal diamond anvil cell[23] was used with diamond type Ia anvils. Details on the precise setup can be found in our previous works.[24,25] The hydrothermal diamond anvil cell (HDAC) apparatus (Fig. 1) consisted of a gasket that contained a small hole ($\sim$ 0.5 mm) that served as the reaction chamber. The reaction chamber was pressed between two diamond anvils that formed the top and bottom of the reactor and also the hydrostatic seal. Each anvil was surrounded by hand-wound MoO microheaters, each having a nominal 1-Ω

TABLE I
Major Reaction Products Identified in Studies on the Treatment of Polyvinylchloride (PVC) with Water under Catalytic and Noncatalytic Conditions

PVC, M_w	Catalyst	Reactor size (mL)	T (°C)	Reaction time (min)	ρ[a] (kg/m^3)	Major reaction products			Max dechlor	Ref. no.
						Solid	Liquid	Gaseous		
65,000	O_2, NaOH	1900	260	24	784	Brown residue	Water soluble organics, benzaldehyde	HCl, CO_2, H_2	100	10
1100^{DOP}	Fe, NaOH	120	300	60	712	nr	nr	Alkanes, CH_4, CO_2	100	11
1100^{DOP}	NaOH	120	400	60	333	nr	nr	Alkanes, CH_4, CO_2	100	11
1100^{DOP}	None	120	400	60	333	nr	More liquid product than subcritical or catalytic cases	Alkanes, CH_4, CO_2	80	11
nr	None	25	450	60	210	nr	Acetic acid, phenol, benzene, butyl phenol, hydroquinone	Propane, butane, pentane	100	12
nr	None	25	600	60	210	nr	Phenol, benzene, naphthalene, hydroquinone	Propane, butane, benzene	100	12
62,000	None	4	370	60	750	Conjugated alkenes, polyenes, non-Cl residue	Benzene, naphthalene, fluorene, indane, toluene, diphenyl-methane, anthracene, biphenyl	nr	100	13
38,000	NaOH	1000	240	120	813	Aromatics, C=O, −OH, =C−H, polyene structures	nr	HCl measured	95–98	14, 15
nr	None	25	400	60	200	Polyene residue at 300°C; none reported at 400°C	Acetone, phenol, benzene, benzoic acid, cyclohexanone, methyl cyclopentane, methyl ethyl ketone	CH_4, CO_2, ethane, benzene, propane, butane, propylene, ethylene, pentene, butylene	100	16

nr: not reported.
[a] Density estimated from either loading conditions or the saturation properties of water.

resistance. The outer assembly of the HDAC allowed the anvils to be pressed against the gasket. Initial pressure in the chamber was adjusted by tightening or loosening the torque on three screws on the HDAC assembly.

The procedure used for alignment of the diamond consisted of three steps as described next. First, the anvils, without gasket, were adjusted using translation of the upper anvil to achieve the maximum area according to light transmission of the microscope. Then, the lower anvil was rotated until Newton rings could be observed. Finally, the alignment was checked by measuring the phase transition of solid AgI, whose details are described in Ref. 26.

The gaskets used in the experiments were $\sim 5 \times 5$ mm^2 and cut from 0.2-mm thick inconel-600 sheet. The gaskets were preindented by applying force from the anvils onto the gasket hole that did not contain sample and this insured minimal change of the gasket shape during the experiments.

Temperature was measured at three points with bare-wire 0.2-mm K-type thermocouples (Omega) with one point being measured on the lower anvil and two points being measured on the upper anvil. The output from one of the upper anvil thermocouples was used for a high-speed temperature controller (RKC Instrument, REX-G9 Series/A, Tokyo) that had a 0.1-s sampling rate with a thyristor voltage of nominally 10 V AC maximum. The output from the other two thermocouples was measured with a data logger (Agilent 34970A, Palo Alto) and computer at a frequently of 2 Hz. Each experiment had associated with it, a heating profile that was kept as uniform as possible between the experimental runs. However, heat up times had to be varied slightly for different target temperatures. The heating profile consisted of a heating segment (90–100 s), in which the contents of the chamber were brought to reaction temperature, a constant temperature segment (500 s), in which contents of the chamber were allowed to react at a given temperature, and a cooling segment (10–20 s), in which electrical power to the heaters was shut off and the contents of the chamber were allowed to cool by convection. The reaction time for the constant temperature segment was the same for all runs. Reliability of the thermocouples was verified to be ± 0.5°C according to the observation of metal melting points of tin (231.9°C) and zinc (419.58°C). Reported temperatures are nominal over the reaction period due to control and drift.

In the experiments, two PVC particles were always used to allow for material variability. PVC particles were loaded into the sample chamber onto the lower anvil while Ar gas was allowed to flow over and around the sample chamber. Then, a droplet of water was placed on the upper anvil of the cell and the two anvils were pressed together. Argon gas trapped in the chamber during this procedure allowed variation of the system density.

Pressures in the cell were estimated by the equation of state of Wagner and Pruss[27] and densities were obtained by using the homogeneous temperature as described in our previous works.[24,25] Briefly, an inert gas, argon, is loaded into the HDAC chamber along with the reactants and water. When heating the materials at constant volume, disappearance of the argon gas bubble provides the temperature that is close to the saturation curve of water.[24] The state point on the saturation boundary provides the overall system density and from this information, the system pressure can be estimated from the equation of state of pure water[27] using the measured temperature and the saturation boundary density.

Direct observations of PVC and water in the chamber during heating were viewed with a microscope (Olympus SZX ZB12, Tokyo) at various magnifications up to 100× and images were captured in real-time with a CCD camera (Olympus CS230, Tokyo). Infrared spectra of the PVC residues after completion of each experiment were performed with an FTIR microscope (JASCO Irtron IRT-30, Tokyo) using 32 scans, 5-s exposure, at 4 cm^{-1} resolution. It should be noted that all analyses performed in this work were for the solid residues.

Definition of spread time

During the initial experiments, we noticed a curious phenomena in which the PVC polymer sample would spread spontaneously within seconds across the anvil according to the reaction time and conditions. Since we found that this spread time seemed to show a regular trend in the initial experiments, we measured its value at all experimental conditions.

The spread time, S_t, was defined as the time at which the polymer particle began to initially wet the lower anvil during under conditions of constant temperature and subsequently spread over the anvil surface. The period of the spreading varied from about 3 s at the highest temperature (500°C) to 15 s at the lowest temperature (400°C) studied. The initial spread times were recorded and these did not vary by more than ± 10 s for similar temperature and density conditions.

Since wetting of a high energy surface by a liquid greatly depends on its physical properties, the spread time, S_t, is related to dechlorination, oxygenation, and cracking reactions occurring in the PVC particles. In other words, the initial spread times allow one to follow the reaction progress and this is illustrated in the next section.

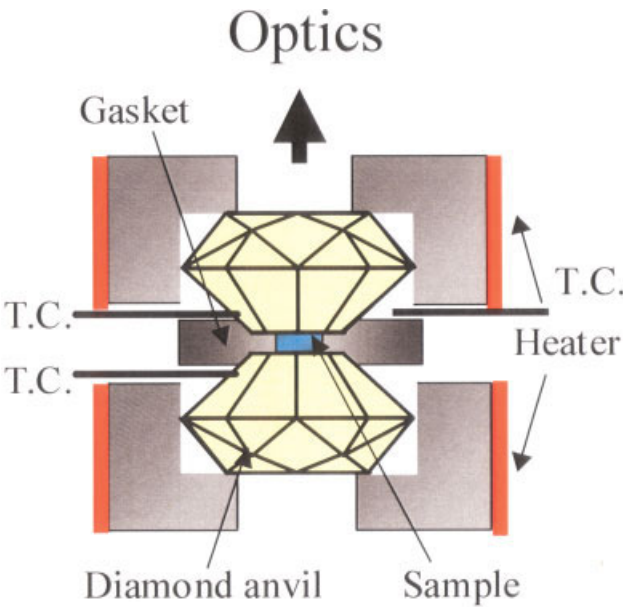

Figure 1 Experimental apparatus. [Color figure can be viewed in the online issue, which is available at www.interscience.wiley.com.]

RESULTS AND DISCUSSION

A summary of the 24 experiments performed is given in Table II. In Table II, reaction temperature, density, pressure, and spread times are listed. Spread times are discussed in detail in a later section. Pressures shown in Table II were estimated from the system density as discussed previously. One experiment was performed in the presence of NaOH.

TABLE II
Experimental Conditions and Observed Spread Times and Phase Transition Phenomena

Run	T (°C)	ρ (kg/m^3)	P (MPa)	Spread time[a] (s)
1	400	0	0.2	231
2		68	16	181
3		571	48	265
4		679	91	306
5		745	144	361
6		783	187	388
7		805	218	401
8		823	246	437
9		833	264	459
10		842	280	477
11		859	313	580
12		930	491	–
13	425	721	149	271
14		832	299	353
15	450	725	181	119
16		828	329	206
17		898	490	256
18		960	688	311
19	500	728	240	64
20		837	421	122
21		880	526	152
22		886	542	181
23		904	594	130
24[b]	400	730	129	550

Heat-up times to reaction temperature were 90, 95, and 100 s for the 400, 450, and 500°C experiments, respectively. Samples remained at the specified reaction temperature for 500 s and were then cooled to room temperature in 10–20 s by convection. Pressures shown were calculated from an equation of state (Ref. 27) as explained in the text.

[a] Spread times are the times of initial wetting of the polymer and surface that were reproducible to within ±10 s. Reacting polymer samples spread over a period of time that was roughly from 3 s at 500°C to 15 s at 400°C and also depended on the density.

[b] In presence of 4*M* NaOH.

Visual appearance of PVC

Heating process

Figure 2 shows heating of PVC and water, in which argon gas is also contained within the reaction chamber to reduce the overall water density of the constant volume system. For this case, the water density was nominally 842 kg/m^3 (Run 10, Table II) and the reaction temperature was 400°C. Samples heated in water all showed the general trends noted here for Figure 2. Initially, two PVC particles could be seen with the aqueous phase and argon gas [Fig. 2(a)]. After heating began, the argon gas disappeared at roughly the saturation pressure of water [Fig. 2(b)] and this allowed estimation of the overall water density from the measured temperature by the Wagner equation of state.[27] Subsequently, the PVC sample changed from solid to liquid at roughly its melting point and the particle swelled in volume [Fig. 2(c)]. Continuation of the heating caused the particles to shrink and the solution to turn yellow as the system reached the beginning of the constant temperature segment [Fig. 2(d)], where for the example shown, the temperature was 400°C after 90 s heat up time and 10 s at the reaction temperature. After a given time at the reaction period, the PVC particles wetted the anvil surface as described next.

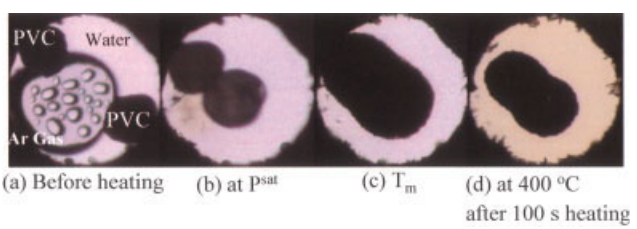

Figure 2 Visual appearance of the chamber during heating (ρ = 842 kg/m^3). See Table II, Run 10 for details. [Color figure can be viewed in the online issue, which is available at www.interscience.wiley.com.]

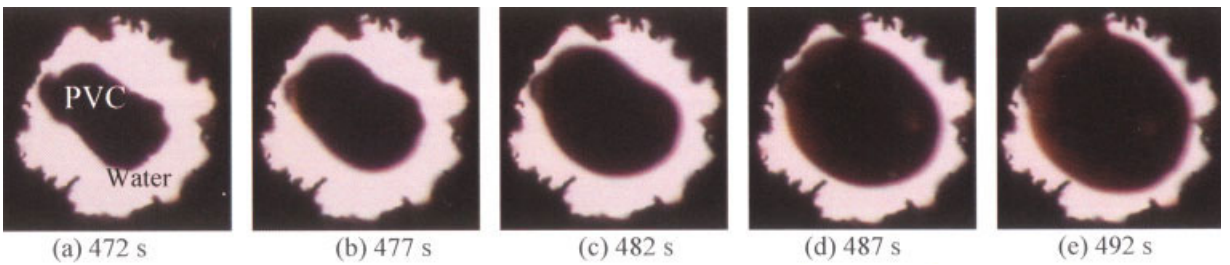

Figure 3 Spread time and spreading phenomena during heating (ρ = 842 kg/m^3). See Table II, Run 10 for details. [Color figure can be viewed in the online issue, which is available at www.interscience.wiley.com.]

PVC spreading phenomena

Figure 3 shows the time evolution of the PVC particles during the reaction period. As heating continued from that shown at 100 s [Fig. 2(d)], the PVC particles shrank [Fig. 3(a)] and then began to change and clearly wet and spread along the anvil surface [Fig. 3(b)]. Wetting of the surface by the polymer continued [Fig. 3(b,d)] and then subsided after about 15 s [Fig. 3(e)]. The period during which spreading occurred was a function of temperature and density and the period tended to decrease with increasing reaction temperature.

Figure 4 shows visual observation of PVC samples being heated in water in which the density of water in each sample chamber was roughly the same value of 830 kg/m^3 (Table II, Runs 10, 16, and 20). For each reaction temperature, the sample is shown for a heating time of 100 s, which is close to the beginning of the reaction period as given in Table II. As the chamber contents were maintained at the reaction temperature, decomposition of the PVC occurred and the sample spread out and wetted the anvil. Figure 4 shows the PVC samples at reaction temperatures of 400, 450, and 500°C just after the spreading occurred. The reaction proceeded as shown by the images at 600 s (Fig. 4), where each mixture changed color with the 400°C sample becoming lighter brown in color and the other samples turning deeper brown or black according to temperature. Gas bubbles appeared during the reaction period for the sample at 400°C, indicating that gas was indeed generated over that of the argon gas added during loading.

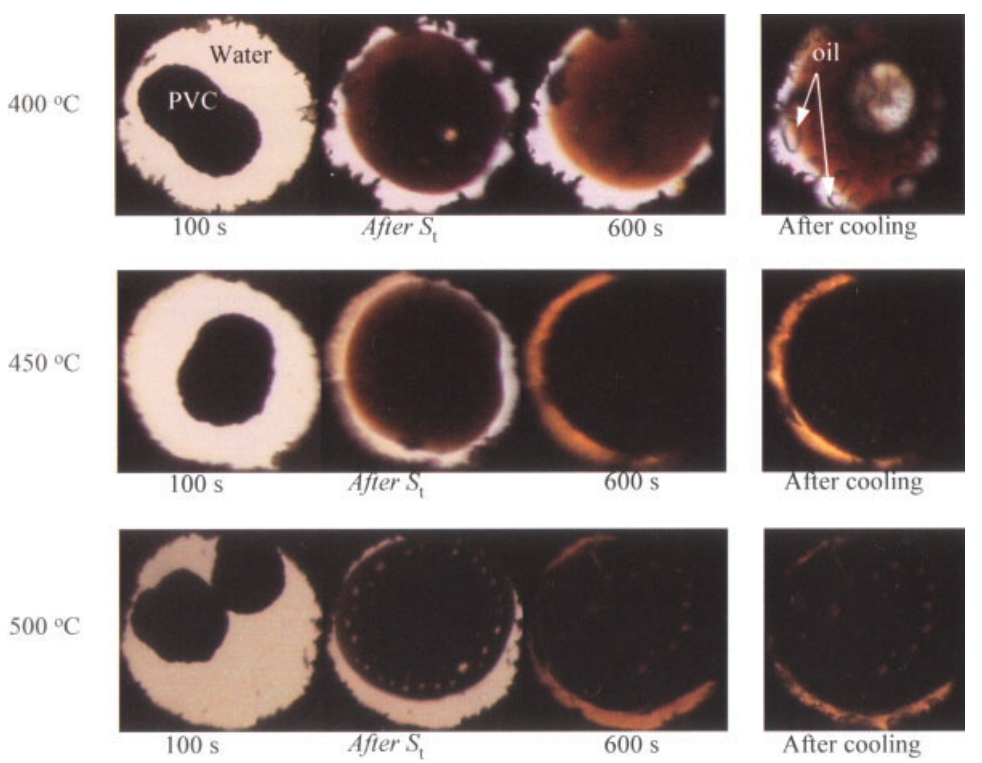

Figure 4 Visual appearance of sample chamber (ρ = $\sim$ 830 kg/m^3). See Table II, Runs 10, 16, and 20 for details. [Color figure can be viewed in the online issue, which is available at www.interscience.wiley.com.]

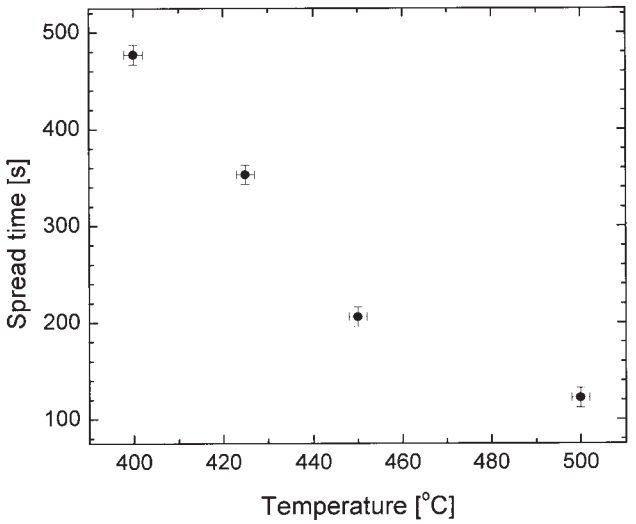

Figure 5 Variation of spread time with reaction temperature for PVC + water mixtures ($\rho = \sim 830$ kg/m^3).

After cooling, oil product appeared in each sample and more gas seemed to be present for the sample reacted at 400°C. Further, oil was visible in the sample at 400°C as shown by the arrows (Fig. 4).

The spread times (Table II, Fig. 4) differed considerably among the experiments at the given temperatures, although the phenomenon of the spreading in itself was similar among the runs. The time in which the wetting initially occurred was denoted as the spread time, as explained in a previous section.

Figure 5 shows the variation of spread times with temperature for experimental runs at approximately the same density. With increasing reaction temperature, the values steadily decreased and seemed to approach an asymptotic value at the highest temperature. This trend can be discussed in terms of surfaces energies, liquid spreading on surfaces, and the underlying reactions that are proceeding.

From the point of view of physical chemistry, surface wetting is related to the surface energy of the contacting phases through the spreading tension, σ^{LSV}, which is based on the Young coefficient for describing contact angle[28]:

$$\sigma^{LSV} = \gamma^{SV} - \gamma^{LV} - \gamma^{LS} \quad (1)$$

where the γ values refer to solid–vapor, liquid–vapor, and solid–liquid contributions of the surface tension. The necessary condition for spreading of a liquid across a surface according to eq. (1) is that the spreading tension be positive. Since diamond has a high free surface energy, spreading of a pure liquid, such as a hydrocarbon, onto a clean dry surface would be expected to be spontaneous.[29] However, in the experiments of this work, the fluid phase consists of supercritical water and this phase would be expected to change the high surface energy of the solid surface, since the state of water is like a dense gas that has strong interactions with all phases. The chemical character of supercritical water is slightly polar, rather than strongly polar, and thus supercritical water is able to dissolve many nonpolar organics including paraffinic hydrocarbons.[30] Thus, although one would not expect there to be strongly adsorbed components onto the solid surface, the surface would be expected to have some of the characteristics of the supercritical water phase. Further, water would be expected to dissolve into the polymer phase.

The area of a spreading of liquid drop over a dry surface depends on the equation for lubrication and can be modeled in terms of Hamaker constant, which describes molecular interactions, the liquid surface tension, the velocity of the spreading liquid, the liquid viscosity and the experimental spread time.[31] The dynamics of a liquid spreading on a solid surface depends on the moving liquid front and has been noted to scale algebraically with the capillary number, Ca, for completely wetting fluids and exponentially for partially wetting fluids.[32] In this work, it is not the intent to perform detailed analyses of the spreading phenomena, since the characteristics of the liquid, including composition, were changing through chemical reaction. However, it is important to point out key variables in the spreading phenomena, with spreading area being directly proportional to the liquid surface tension and inversely proportional to the liquid viscosity.[31]

Consider the effect of the polymer molecular weight on the properties, surface tension and viscosity. For the case of polystyrene, in the range of molecular weights less than $\sim$ 50,000 g/mol, surface tension changes greatly with molecular weight and shows a large increase with molecular weight, whereas for molecular weights greater than this value, the surface tension is a weak function of molecular weight.[33] On the other hand, for the case of polystyrene as well as many polymers, molecular weight shows a log–log relationship with viscosity.[34] From this information, the following conclusions can be drawn. For a polymer with a moderately high molecular weight ($\sim$ 50,000 g/mol), changes in molecular weight will not affect the surface tension so much, whereas there will be large changes in the viscosity. As the molecular weight of a polymer decreases, it should be much more likely to achieve the conditions for spreading spontaneously on a high energy surface. Further, chlorination in a compound generally causes both the surface tension to increase and viscosity to increase,[29] and therefore, dechlorination of PVC should cause both surface tension and viscosity to decrease, making spreading more likely to occur as the reaction proceeds.

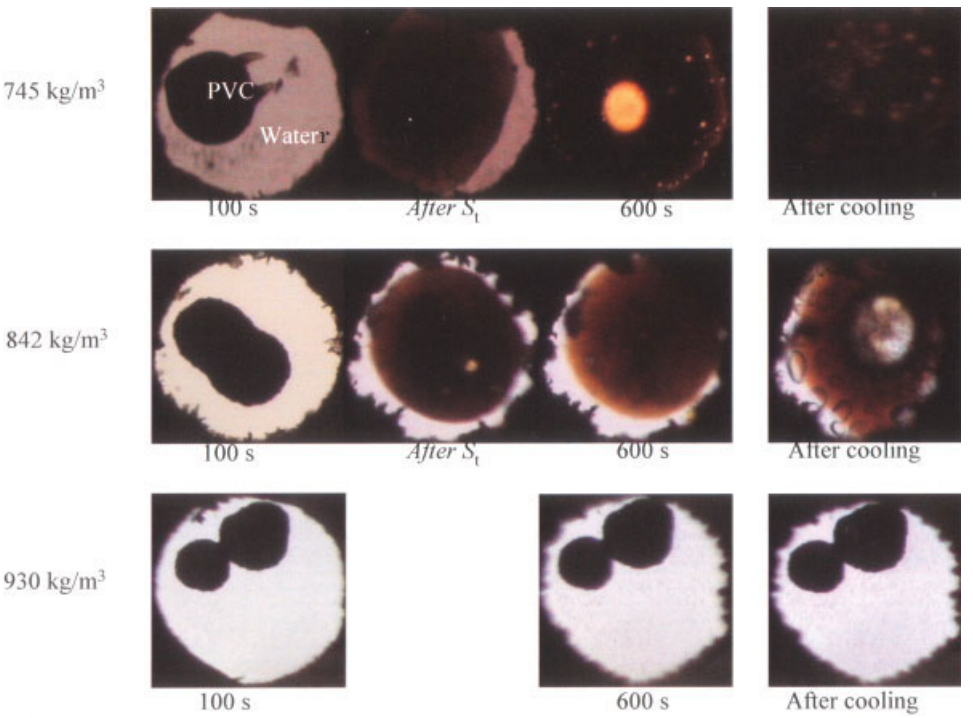

Figure 6 Visual appearance of sample chamber (400°C). See Table II, Runs 5, 10, and 12 for details. [Color figure can be viewed in the online issue, which is available at www.interscience.wiley.com.]

The PVC spreading can be understood as follows. First, at the reaction temperature, PVC spreading did not occur spontaneously but required some time. In other words, chemical reaction had to occur to decrease the molecular weight for the spreading to become favorable according to eq. (1). This is true for all cases, including the case for reaction of PVC without water (Table II, Run 1). As the reaction proceeded (Fig. 4), alkene C=C bonds, that is, polyenes, were generated as dechlorination of the reactant occurred. The color changes observed for the PVC particles are indicative of the chlorine removal process as noted by Gokcel et al.,[35] who found that PVC progressively undergoes color changes from yellow, orange, red, brown, and black depending on the number of conjugated double bonds formed during dechlorination. Moreover, it is clear from the example shown earlier [Fig. 2(d)] that the aqueous phase changed into a yellow color, and that corrosion products appeared around the periphery of the reactor and grew as the reaction continued [Fig. 3(a–e)], both of which are indicative of progress of the dechlorination. As the chlorine content of the PVC decreased, the surface tension and viscosity would also be expected to decrease. Cracking reactions also would be expected to occur as has been shown for water–polyethylene systems,[36] and this would lower the polymer molecular weight and reduce its viscosity. As shown in Figure 5, spread times became shorter as reaction temperature was increased and this is clear evidence that both dechlorination and cracking reactions were accelerated at high temperatures at the given water density.

Water density as well as reaction temperature can be expected to affect reaction rates and spread times. Figure 6 shows the visual appearance of the sample chamber at water densities of 745, 842, and 930 kg/m^3 (Table II, Runs 5, 10, 12), where the reaction temperature of each sample was 400°C. At 745 and 842 kg/cm^3, spread times could be observed and measured as expected and increased substantially with increasing water density. At 930 kg/m^3, the PVC particle did not change and also did not spread on the surface within the combined heat-up and reaction time of 600 s. Smith et al.[37] have noted for nylon 6/6 that high hydrostatic pressures ($\sim$ 900 MPa) on polymers can greatly change both the melting and reaction characteristics of the polymers due to changes in both crystallinity of the polymer and polymer–water interactions. For the case shown in Figure 6, the calculated pressure was 491 MPa, which can be considered high. Since the temperature was well above the melting point of the polymer, the lack of spread time within the reaction period was probably due to the high density conditions that suppressed both cracking and dechlorination reactions. At supercritical temperatures, the properties of water change from those that favor radical reaction pathways at low density to those that favor ionic reactions at high density, as discussed in Watanabe

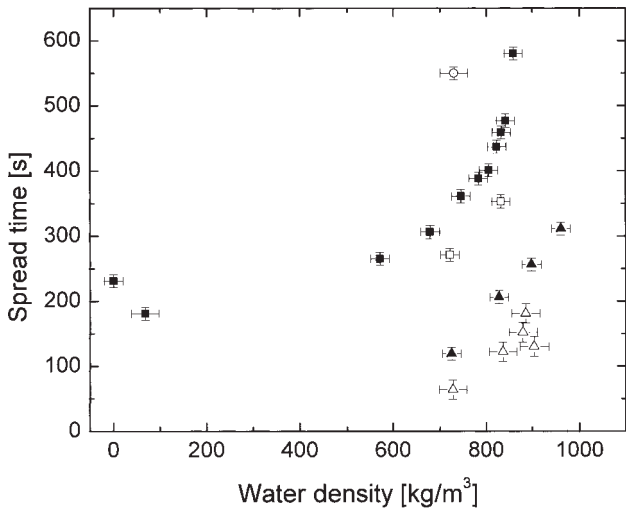

Figure 7 Effect of water density on spread time for all experiments noted in Table II. Symbols: filled squares, 400°C; open squares, 425°C; filled triangles, 450°C; open triangles, 500°C; single open circle, 400°C with 4*M* NaOH.

et al.[22] Since the PVC sample at the highest density (Fig. 6) did not exhibit strong changes in shape or color, this is probably a strong evidence that the reaction pathways at high water densities were ionic in nature. Further evidence for the lack of reactivity of the PVC at the highest density (Fig. 6) can be seen by the cooled samples, which showed only small changes in appearance compared with the other samples after cooling (Fig. 6).

The spread times measured at 400°C along with all other runs in Table II were plotted versus water density as shown in Figure 7. Considering the data at 400°C (Fig. 7), spread times became longer with increasing water density, which is evidence that dechlorination and cracking reactions were inhibited. Both dechlorination and cracking reactions were most likely accelerated at low densities according to visual observations and the variation in the spreading times. At the lowest water density of 68 kg/m^3 (Table II, Run 2), the spread time decreased to a low value of 181 s, when compared with zero water density or high density values at 400°C reaction temperature. For the reaction performed in the absence of water (Table II, Run 1), the spread time was just at the melting point of the polymer, as would be expected according to eq. (1). Further, formation of polyene structures can be followed with viscometry as has been reported in the literature.[38]

At all temperatures, correlation of the spread time with water density was found. From the observed spread times, it can be concluded that dechlorination and cracking reactions are promoted at low densities and high temperatures, and conversely, these reactions are inhibited at high densities and low temperatures.

One experiment was made in the presence of NaOH, since it has been reported in the literature that caustic solutions heated with PVC promote dechlorination in high temperature water.[8,9] As shown in Figure 7, the spread time was high for this run, which implies that although the dechlorination rate of PVC with NaOH may be relatively high, polymer degradation was inhibited. NaOH neutralizes the HCl generated and lowers catalytic effects similar to that observed for other bases[39] in the supercritical water. Further, the neutralization generates salt, which may act to inhibit hydrolysis.

Another factor that should be considered when interpreting the spread time data is the evolution of HCl during the dechlorination reaction. Hjertberg and Sorvik[38] noted that for HCl concentrations less than 10%, the rate of PVC dehydrochlorination is mainly due to propagation rate, whereas for higher HCl concentrations ($\sim$ 10%), an increase in initiation rate was proposed, which leads to an autoacceleration effect in PVC dehydrochlorination. In a related work, Hjertberg et al.[40] found that an increase in HCl concentration not only increases the initiation rate, but also can lead to shorter polyene segments. In the presence of water, the effect of HCl on PVC dechlorination can be expected to be much less than for HCl vapor phase for several reasons. First, when there is an aqueous phase present, the HCl generated during PVC dechlorination is rapidly removed from the polymer phase as discussed by Endo and Emori[41] for high-temperature water. Second, as the water to PVC ratio is relatively high, the concentrations of HCl are estimated to be relatively low. Third, the ionization of a strong acid can be expected to be less than that in water at room temperature,[42,43] since the dielectric constant of at supercritical temperatures and at pressures of this work range from 14 to 20 as shown by data[44] and correlations[45] in the literature. Therefore, one can expect the catalytic effect of HCl on the reaction to be lower than that of HCl in the vapor phase. On the other hand, due to the properties of water, one can expect strong temperature and density effects on the reaction pathways and reaction rates.

IR spectra of solid product

Figure 8 shows infrared spectra of sample residues at a water density of $\sim$ 830 kg/m^3. The following spectra positions are noted: —OH stretching vibrations from 3200 to 3600 cm^{-1}, =C—H stretching vibrations related to aromatics or unsaturated fatty acids from 3000 to 3100 cm^{-1}, —C—H stretching vibrations related to a saturated fatty acid from 2800 to 3000 cm^{-1}, and C=C stretching vibrations at 1610 cm^{-1}. Comparing the spectra of the residue at 400°C with that of standard PVC (Fig. 8), OH stretching

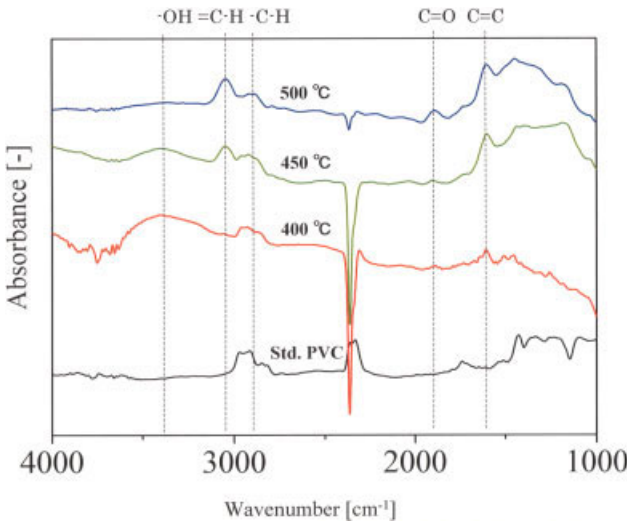

Figure 8 Infrared spectra of solid products ($\rho = \sim 830$ kg/m^3). See Table II, Runs 10, 14, and 20 for details. [Color figure can be viewed in the online issue, which is available at www.interscience.wiley.com.]

appeared at 400°C and gradually decreased with increasing temperature, whereas =C—H stretching increased with increasing temperature. At all conditions, C=C bonds were generated.

Figure 9 shows infrared spectra of residues obtained by reaction at 400°C (Fig. 6) with spectral positions marked for the various contributions as in Figure 8. As shown in Figure 9, OH bonds just began to appear at the lowest water density of 750 kg/m^3, and as the density increased, the OH stretching became stronger. At the lowest density, the =C—H stretching was strongest among the residues. Similar to the previous constant density case

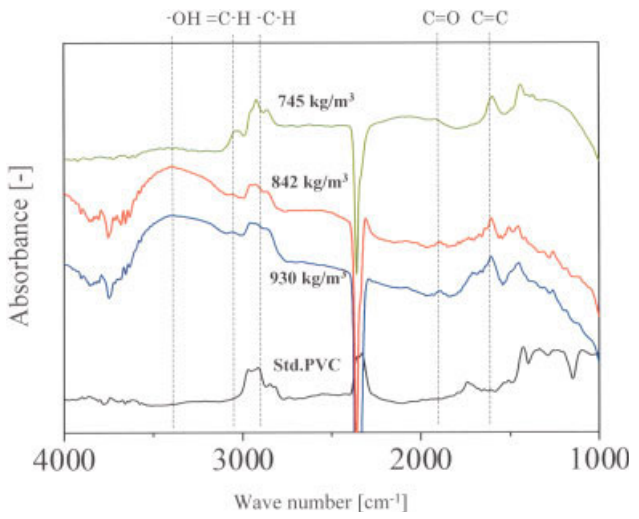

Figure 9 Infrared spectra of solid products (400°C). See Table II, Runs 5, 10, and 12 for details. [Color figure can be viewed in the online issue, which is available at www.interscience.wiley.com.]

(Fig. 8), C=C bonds were generated at all conditions (Fig. 9).

Reaction mechanism of PVC in supercritical water

The data in the previous sections on visual observations, spread times, and spectral analyses can now be assembled to examine the reaction pathway for PVC decomposition in supercritical water and its variation with temperature and density. First, aspects of the PVC dechlorination mechanism are discussed with respect to thermal degradation in the absence of water.

There is a fair amount of debate in the literature on the dechlorination of PVC during thermal degradation with respect to mechanistic aspects of dechlorination initiation, propagation, termination steps, and subsequent polyene formation at lower temperatures around 180°C.[46,47] Starnes and Ge[46] report on the mechanism of autocatalysis in the thermal dehydrochlorination of PVC and show that the autocatalysis is free-radical with respect to abstraction of hydrogen and nonfree radical in the generation of polyene sequences. Starnes also provides a comprehensive review on most of the current proposals for the dehydrochlorination mechanism of PVC[47] and summarizes the main process of the thermal degradation of PVC as being one of chain reaction with initiation and propagation steps occurring exclusively via ion pairs or transition states that are highly polarized along with termination steps. As discussed in the previous section, however, the effect of the properties of water on the reaction is expected to dominate the reaction paths.

Figure 10 shows a proposed reaction pathway for PVC degradation in water that is estimated from results in this work and discussed with respect to temperature and density effects. At zero water density and at high temperatures (>400°C), PVC degradation proceeds through **1** then **3** via ionic chain reaction as discussed earlier and through cracking, which generates aromatic and low molecular weight

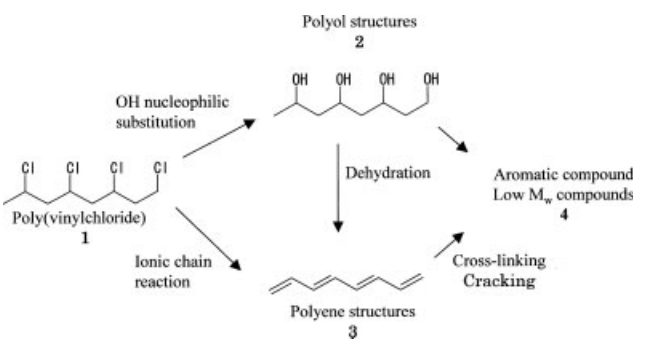

Figure 10 Reaction pathway of polyvinylchloride decomposition in high temperature and supercritical water.

compounds **4**. As water is added to the system, OH nucleophilic substitution occurs competitively with ionic pair dechlorination to form polyol structures **2**. Cracking and hydrolysis occur, which lower the spread time to its minimum value at water density of 68 kg/m^3 (Fig. 7) at 400°C. As water density is increased to above its value at the critical point (ρ_c = 322 kg/m^3), OH nucleophilic substitution reaction is accelerated with increasing water density as shown by the IR analyses in the previous section (Fig. 9). At water densities greater than ρ_c, increasing temperature leads to a lower rate of polyol **2** formation (Fig. 8) that can be attributed to (i) increased reactivity of polyene structures formed, (ii) dehydration of polyol structures **2** to yield polyene structures **3**, and (iii) probable decomposition and hydrolysis of polyol structures **2** to lower molecular weight compounds **4**, such as tri-, di-, propylene glycols that break down to hydroxyacetone as reported by Dai et al.[48] Considering the spread time data and spectral analyses, the OH nucleophilic substitution reaction pathway was promoted at low temperatures (ca. <450°C) and high water densities (ca. >830 kg/m^3).

In all runs, C=C bond stretches associated with polyene structures were observed and their absorbance values were somewhat larger with increasing temperature directly (Fig. 8). However, the amount of polyene structures formed as judged by the absorbance values were lower than expected, which can be attributed to formation of polyol structures **2** (Fig. 8) and increased reactivity of the polyene structures **3** formed along with cracking reactions that generate gas products, especially at low water densities.[12,16] Considering the spread time data and spectral analyses, the ionic chain reaction pathway was promoted at high temperatures ($> \sim 450$°C) and low water densities ($< \sim 750$ kg/m^3).

CONCLUSIONS

In this work, we examined the degradation of PVC in water at high temperatures and high pressures with a HDAC. The following conclusions can be reached. In the heating of PVC in water, the polymer undergoes spreading that is clear and abrupt according to reaction time, temperature, and solvent conditions. The spread time of the degrading PVC correlates with both temperature and water density. High temperatures tend to lower spread time, while high water densities increase spread time. The spread time seems to be strongly related to the extent of reaction and also to the degree of dechlorination. Polyene structures are formed at all conditions studied for the range of reaction times ($\sim$ 500 s), temperatures (400°C $> T >$ 500°C), and water densities (<930 kg/m^3). At high temperatures ($> \sim 450$°C) and low water densities ($< \sim 750$ kg/m^3), ionic chain reactions seem to be promoted, which lead to polyene structures. At high water densities ($> \sim 830$ kg/m^3), polyol structures are formed, which is probably due to OH nucleophilic substitution by water. The polyol structures seem to be promoted at low temperatures ($< \sim 450$°C) and at high densities ($> \sim 830$ kg/m^3). More gas seems to form at low temperature ($\sim$ 400°C) than at high temperature conditions (500°C), which can probably be attributed to the effect of the water density on the polyene decomposition. A reaction pathway is proposed that shows competitive formation of polyols and polyenes in water according to the temperature and density of water. Future work will examine the pathway in more detail via *in situ* spectroscopic methods and will study the effect of HCl concentration on the polyol formation.

References

1. Braun, D. J Vinyl Additive Technol 2001, 7, 168.
2. Braun, D. J Polym Sci Part A: Polym Chem 2004, 42, 578.
3. Production: Growth in most regions. C & E News, July 11, 2005, p 67.
4. Braun, D. Prog Polym Sci (Oxford) 2002, 27, 2171.
5. Howell, B. A. J Therm Anal Calorimetry 2006, 83, 53.
6. Brandrup J.; Immergut, E. H.; Grulke, E. A.; Abe, A.; Bloch, D. R., Eds. Polymer Handbook, 4th ed.; Wiley: New York, 1999; p VI–545.
7. Bhaskar, T.; Negoro, R.; Muto, A.; Sakata, Y. Green Chem 2006, 8, 697.
8. Yoshioka, T.; Furukawa, K.; Sato, T.; Okuwaki, A. J Appl Polym Sci 1998, 70, 129.
9. Shin, S. M.; Yoshioka, T.; Okuwaki, A. Polym Degrad Stab 1998, 61, 349.
10. Sorensen, E.; Bjerre, A. B. Waste Manage 1992, 12, 349.
11. Enomoto, H.; Hatakeyama, A.; Kato, Y. Haikibutsu Gakkai Ronbunshi 1995, 6, 16.
12. Sato, Y.; Kato, K.; Takeshita, Y.; Takahashi, K.; Nishi, S. Jpn J Appl Phys Part 1 1998, 37, 6270.
13. Kubatova, A.; Lagadec, A. J. M.; Hawthorne, S. B. Environ Sci Technol 2002, 36, 1337.
14. Lu, J.; Ma, S.; Gao, J. Energy Fuels 2002, 16, 1251.
15. Lu, J.; Ma, S.; Gao, J.; Freitas, J. C. C.; Bonagamba, T. J. J Appl Polym Sci 2003, 90, 3252.
16. Takeshita, Y.; Kato, K.; Takahashi, K.; Sato, Y.; Nishi, S. J Supercrit Fluids 2004, 31, 185.
17. Lemmon, E. W.; McLinden, M. O.; Friend, D. G. In Thermophysical Properties of Fluid Systems in NIST Chemistry Webbook; Linstrom, P. J., Mallard, W. G., Eds.; National Institute of Standards and Technology: Gaithersburg, MD, 2005; NIST standard reference database number 69. Available at http://webbook.nist.gov/chemistry (accessed Oct 21, 2006).
18. Arai, K.; Adschiri, T. Fluid Phase Equilib 1999, 158–160, 673.
19. Bröll, D.; Kaul, C.; Krämer, A.; Krammer, P.; Richter, T.; Jung, M.; Vogel, H.; Zehner, P. Angew Chem Int Ed 1999, 38, 2998.
20. Savage, P. E. Chem Rev 1999, 99, 603.
21. Weingärtner, H.; Franck, E. U. Angew Chem Int Ed 2005, 44, 2672.
22. Watanabe, M.; Sato, T.; Inomata, H.; Smith, R. L., Jr.; Arai, K.; Kruse, A.; Dinjus, E. Chem Rev 2004, 104, 5803.

23. Bassett, W. A.; Shen, A. H.; Bucknum, M.; Chou, I. M. Rev Sci Instrum 1993, 64, 2340.
24. Ogihara, Y.; Smith, R. L., Jr.; Inomata, H.; Arai, K. Cellulose 2005, 12, 595.
25. Fang, Z.; Smith, R. L., Jr.; Inomata, H.; Arai, K. J Supercrit Fluids 1999, 15, 229.
26. Bassett, W. A.; Takahashi, T. Am Mineral 1965, 50, 1576.
27. Wagner, W.; Pruss, A. J Phys Chem Ref Data 2002, 31, 387.
28. Adamson, A. W. Physical Chemistry of Surfaces, 5th ed.; Wiley: New York, 1990.
29. Fox, H. W.; Hare, E. F.; Zisman, W. A. J Phys Chem 1955, 59, 1097.
30. Ikushima, Y.; Hatakeda, K.; Saito, N.; Arai, M. J Chem Phys 1998, 108, 5855.
31. Starov, V. M.; Kalinin, V. V.; Chen, J. D. Adv Colloid Interface Sci 1994, 50, 187.
32. Kalliadasis, S.; Chang, H. C. Ind Eng Chem Res 1996, 35, 2860.
33. Moreira, J. C.; Demarquette, N. R. J Appl Polym Sci 2001, 82, 1907.
34. Rodriguez, F. Principles of Polymer Systems, 4th ed.; Taylor & Francis: Washington, DC, 1996.
35. Gokcel, H. I.; Balkose, D.; Kokturk, U. Eur Polym J 1999, 35, 1501.
36. Fang, Z.; Smith, R. L., Jr.; Inomata, H.; Arai, K. J Supercrit Fluids 2000, 16, 207.
37. Smith, R. L., Jr.; Fang, Z.; Inomata, H.; Arai K. J Appl Polym Sci 2000, 76, 1062.
38. Hjertberg, T.; Sorvik, E. M. J Appl Polym Sci 1978, 22, 2415.
39. Johnston, K. P.; Chlistunoff, J. B. J Supercrit Fluids 1998, 12, 155.
40. Hjertberg, T.; Martinsson, E.; Sorvik, E. Macromolecules 1988, 21, 603.
41. Endo, K.; Emori, N. Polym Degrad Stab 2001, 74, 113.
42. Chlistunoff, J.; Ziegler, K. J.; Lasdon, L.; Johnston, K. P. J Phys Chem A 1999, 103, 1678.
43. Johnston, K. P.; Bennett, G. E.; Balbuena, P. B.; Rossky, P. J. J Am Chem Soc 1996, 118, 6746.
44. Fernandez, D. P.; Goodwin, A. R. H.; Lemmon, E. W.; Levelt Sengers, J. M.; Williams, R. C. J Phys B 1997, 26, 1125.
45. Uematsu, M.; Franck, E. U. J Phys Chem Ref Data 1980, 9, 1291.
46. Starnes, W. H., Jr.; Ge, X. Macromolecules 2004, 37, 352.
47. Starnes, W. H., Jr. Prog Polym Sci (Oxford) 2002, 27, 2133.
48. Dai, Z.; Hatano, B.; Tagaya, H. Polym Degrad Stab 2003, 80, 353.